Molecular Pharmacology Fast Forward. Published on June 21, 2013 as doi:10.1124/mol.113.086835
This article has not been copyedited and formatted. The final version may differ from this version.

Potent Inhibition of Aldehyde Dehydrogenase-2 by Diphenyleneiodonium: Focus on Nitroglycerin Bioactivation

Regina Neubauer, Andrea Neubauer, Gerald Wölkart, Christine Schwarzenegger, Barbara Lang, Kurt Schmidt, Michael Russwurm, Doris Koesling, Antonius C.F. Gorren, Astrid Schrammel and Bernd Mayer

Department of Pharmacology and Toxicology, Karl-Franzens-Universität Graz, Austria (R.N., A.N., G.W., C.S., B.L., K.S., A.C.F.G., A.S., B.M.)

Department of Pharmacology and Toxicology, Ruhr-Universität Bochum, Germany (M.R., D.K.)

Molecular Pharmacology Fast Forward. Published on June 21, 2013 as DOI: 10.1124/mol.113.086835
This article has not been copyedited and formatted. The final version may differ from this version.

Running Title: Inhibition of ALDH2 by diphenyleneiodonium

Address Correspondence to:

Dr. Bernd Mayer

Department of Pharmacology and Toxicology

Karl-Franzens-Universität Graz

Universitätsplatz 2, A-8010 Graz, Austria

Tel.: +43-316-380-5567

Fax: +43-316-380-9890

e-mail: mayer@uni-graz.at

Number of text pages: 29

Number of tables: 0

Number of figures: 6

Number of references: 39

Number of words in

Abstract: 247

Introduction: 714

Discussion: 879

[1]Abbreviations: ALDH, aldehyde dehydrogenase; ADH, alcohol dehydrogenase; DEA/NO, 2,2-diethyl-1-nitroso-oxyhydrazine; EDTA, ethylene diamine tetraacetic acid; DIP, diphenyliodonium; DMSO; dimethyl sulfoxide; DPI, diphenyleneiodonium; DTPA; dieethylene triamine pentaacetic acid; DTT, dithiothreitol; GDN, glycerol dinitrate; GTN, glycerol trinitrate (nitroglycerin); NAD, nicotinamide adenine dinucleotide; NO, nitric oxide; sGC, soluble guanylate cyclase.

Molecular Pharmacology Fast Forward. Published on June 21, 2013 as DOI: 10.1124/mol.113.086835
This article has not been copyedited and formatted. The final version may differ from this version.

Abstract

Aldehyde dehydrogenase-2 (ALDH2) catalyzes vascular bioactivation of the antianginal drug nitroglycerin (GTN) to yield nitric oxide (NO) or a related species that activates soluble guanylate cyclase (sGC), resulting in cGMP-mediated vasodilation. Accordingly, established ALDH2 inhibitors attenuate GTN-induced vasorelaxation *in vitro* and *in vivo*. However, the ALDH2 hypothesis has not been reconciled with early studies demonstrating potent inhibition of the GTN response by diphenyleneiodonium (DPI), a widely used inhibitor of flavoproteins, in particular NADPH oxidases. We addressed this issue and investigated the effects of DPI on GTN-induced relaxation of rat aortic rings and the function of purified ALDH2. DPI (0.3 µM) inhibited the high affinity component of aortic relaxation to GTN without affecting the response to NO, indicating that the drug interfered with GTN bioactivation. Denitration and bioactivation of 1 - 2 µM GTN, assayed as 1,2-glycerol dinitrate formation and activation of purified sGC, respectively, were inhibited by DPI with a half-maximally active concentration of about 0.2 µM in a GTN-competitive manner. Molecular modeling indicated that DPI binds to the catalytic site of ALDH2, and this was confirmed by experiments showing substrate-competitive inhibition of the dehydrogenase and esterase activities of the enzyme. Our data identify ALDH2 as highly sensitive target of DPI and explain inhibition of GTN-induced relaxation by this drug observed previously. In addition, the data provide new evidence for the essential role of ALDH2 in GTN bioactivation and may have implications to other fields of ALDH2 research, such as hepatic ethanol metabolism and cardiac ischemia/reperfusion injury.

Molecular Pharmacology Fast Forward. Published on June 21, 2013 as DOI: 10.1124/mol.113.086835
This article has not been copyedited and formatted. The final version may differ from this version.

Introduction

It is well established that the organic nitrate nitroglycerin (GTN[1]) is a prodrug that is bioactivated to yield NO or a related reactive species which activates soluble guanylate cyclase (sGC) in vascular smooth muscle, resulting in cGMP-mediated vasodilation. The enzymatic pathway involved in GTN bioactivation has remained elusive for several decades, but in 2002 Stamler and coworkers provided the first evidence that vascular aldehyde dehydrogenase-2 (ALDH2) activity is essential for GTN bioactivity (Chen et al., 2002). This was later confirmed with ALDH2-deficient blood vessels in which the high-affinity pathway of GTN-induced relaxation is absent (Chen et al., 2005). The main route of ALDH2-catalyzed denitration of GTN yields 1,2-glycerol dinitrate (1,2-GDN) and inorganic nitrite, but a minor reaction results in direct formation of NO (Wenzl et al., 2011). Although direct NO formation by ALDH2 observed with the purified enzyme is likely to explain vascular GTN bioactivity, it remains to be shown that this reaction does indeed mediate GTN-induced relaxation of blood vessels.

Long-term administration of GTN results in progressive loss of vascular sensitivity to the nitrate. Several mechanisms were proposed to explain this nitrate tolerance (Fung, 2004), but diminished bioactivation of GTN by ALDH2 appears to be the most plausible cause (Münzel et al., 2011). Vascular ALDH2 activity is reduced in all models of nitrate tolerance, including the unexpected hyposensitivity to GTN observed in ascorbate deficiency (Wenzl et al., 2009b), and ALDH2-deficient mice do not develop tolerance (Chen et al., 2005; Wenzel et al., 2008). However, Bennett and coworkers reported that the residual GTN-induced relaxation of tolerant blood vessels is still sensitive to ALDH2 inhibitors (DiFabio et al., 2003) and that the hemodynamic effects of GTN recovered more rapidly than ALDH activity after nitrate treatment (D'Souza et al., 2011), questioning the key role of ALDH2 inactivation in the development of nitrate tolerance.

Molecular Pharmacology Fast Forward. Published on June 21, 2013 as DOI: 10.1124/mol.113.086835
This article has not been copyedited and formatted. The final version may differ from this version.

Before the essential role of ALDH2 became evident, numerous other pathways have been proposed to explain GTN-induced vasodilation. Among others, GSH-S-transferase, old yellow enzyme, xanthine oxidase, cytochrome P450, and cytochrome P450 reductase were discussed as potential candidates (Fung, 2004). These proposals were almost exclusively based on inhibition of the GTN response by established enzyme inhibitors, and we wondered how these early results could be reconciled with the current knowledge on ALDH2-catalyzed GTN bioactivation. The aryliodonium compound diphenyleneiodonium (DPI) is of particular interest. The drug was described as potent inhibitor of GTN-induced relaxation of isolated rat aorta with submicromolar potency (McGuire et al., 1994) and was shown to reduce the blood pressure response to GTN upon *in vivo* administration (McGuire et al., 1998).

DPI and the related compound diphenyliodonium (DIP) are widely used to probe cells and tissues for NADPH oxidase-derived superoxide and oxidative stress-related processes. It has been proposed that DPI inhibits NADPH oxidase by a turnover-dependent radical mechanism that results in covalent phenylation of the flavin cofactor (O'Donnell et al., 1993). A similar mechanism was described for inhibition of cytochrome P450 reductase (Tew, 1993), and numerous papers published in the past two decades indicate that DPI is a non-selective inhibitor of NAD(P)H-dependent enzymes using flavins as redox cofactors (Aldieri et al., 2008). These include NO synthases, mitochondrial complex I, cytochrome P450 reductase, xanthine oxidase and, described recently, the related molybdo-flavoprotein aldehyde oxidase (Kundu et al., 2012). The affinity constants found in the literature vary from 50 nM to 2.8 mM, with IC_{50} values in the range of 0.3 - 5.6 µM for inhibition of NADPH oxidase (Aldieri et al., 2008). Based on these results, aryliodonium compounds are generally viewed as flavoprotein inhibitors and there is not much evidence for interference of DPI with enyzmatic reactions not involving flavin-mediated electron transfer. Notable exceptions are NAD(P)-dependent metabolic

Molecular Pharmacology Fast Forward. Published on June 21, 2013 as DOI: 10.1124/mol.113.086835
This article has not been copyedited and formatted. The final version may differ from this version.

enzymes and ion channels that are inhibited with IC_{50} values ranging from 3 to 50 µM (Aldieri et al., 2008).

In the present study we show that DPI potently inhibits all enzymatic functions of ALDH2, including denitration and bioactivation of GTN. Substrate-competitive inhibition and docking of DPI to the crystal structure of ALDH2 suggest that DPI binds with high affinity to the catalytic site of the enzyme. Our data explain the inhibition of GTN-induced vasodilation by DPI reported previously and reinforce the essential role of ALDH2 in GTN vasoactivity. Considering the role of ALDH2 in hepatic metabolism of ethanol and cardiac protection, the results may have implications beyond organic nitrate pharmacology.

Molecular Pharmacology Fast Forward. Published on June 21, 2013 as DOI: 10.1124/mol.113.086835
This article has not been copyedited and formatted. The final version may differ from this version.

Materials and Methods

Materials

Bovine lung sGC was purified as previously described (Russwurm and Koesling, 2005). Human ALDH2 was expressed in Escherichia coli BL21 (DE3) and purified as described previously (Beretta et al., 2008; Zheng et al., 1993). Concentrations are expressed per monomer, assuming a molecular mass of 54 kDa. Sephacryl S-300 HR was obtained from GE Healthcare Europe GmbH (Vienna, Austria). NADPH was from Pharma Waldhof (Düsseldorf, Germany). Antibiotics and fetal calf serum were purchased from PAA Laboratories (Linz, Austria). Ethylenediamine tetraacetic acid (EDTA)-free Complete® Protease Inhibitor Cocktail Tablets were from Roche Diagnostics GmbH (Vienna, Austria). [α-^{32}P]GTP (800 Ci/mmol) was from PerkinElmer Life and Analytical Sciences (Vienna, Austria). [2-^{14}C]GTN (50 mCi/mmol) was from American Radiolabeled Compounds, purchased through Hartmann Analytic GmbH (Braunschweig, Germany). Nitro POHL® ampoules (G. Pohl-Boskamp GmbH & Co., Hohenlockstedt, Germany), containing 4.4 mM GTN in 250 mM glucose, were obtained from a local pharmacy and diluted with distilled water. Unlabelled organic nitrates used as standards in radio thin layer chromatography (GTN, 1,2-GDN and 1,3-GDN) were purchased from LGC Standards (Wesel, Germany). 2,2-Diethyl-1-nitroso-oxyhydrazine (DEA/NO) was from Enzo Life Sciences (Lausen, Switzerland) purchased through Eubio (Vienna, Austria). Stock solutions were prepared in 100 mM NaOH and diluted in 10 mM NaOH. All other chemicals and culture media were from Sigma-Aldrich (Vienna, Austria), including DPI, DIP, and alcohol dehydrogenase (ADH) from *Saccharomyces cerevisiae*. DPI and DIP stock solutions were prepared in dimethyl sulfoxide (DMSO).

Molecular Pharmacology Fast Forward. Published on June 21, 2013 as DOI: 10.1124/mol.113.086835
This article has not been copyedited and formatted. The final version may differ from this version.

Animals

Sprague-Dawley rats (obtained from Charles River, Sulzfeld, Germany) of either sex were housed at the local animal facility in approved cages and kept on a regular 12-hour dark/light cycle. They were fed standard chow (Altromin 3023; obtained from Königshofer Futtermittel (Ebergassing, Austria)) and received water *ad libitum*. For the study, they were randomly assigned to two experimental groups. In one group nitrate tolerance was induced by subcutaneous injections of GTN (4 times a day; daily dose 50 mg/kg) for 3 days as previously described (Wölkart et al., 2008), while the other group was left untreated (control group). Animals were euthanized in a box that was gradually filled with CO_2 until no more vital signs (cessation of respiration and circulation) were noticed. Subsequently, the thorax of the animals was opened and the thoracic aorta removed, placed in chilled buffer, and immediately used for functional studies. All animal experiments were performed in compliance with the Austrian law on experimentation with laboratory animals (last amendment 2012), and were approved by Austrian government authorities.

Aortic ring experiments

The thoracic aorta was carefully cleaned from connective tissue and cut into rings of ~3 mm length. For isometric tension measurements the rings were suspended in 5-ml organ baths containing oxygenated Krebs-Henseleit buffer (concentrations in mM: NaCl 118.4, $NaHCO_3$ 25, KCl 4.7, KH_2PO_4 1.2, $CaCl_2$ 2.5, $MgCl_2$ 1.2, D-glucose 10.1; pH 7.4), as previously described in detail (Wölkart et al., 2008). Tissues were equilibrated for 60 min by repeatedly adjusting tension to 1 g and changing the bath solution. Viability of the preparations was then assessed by replacing the bathing solution with a depolarizing buffer containing 100 mM K^+ (taken as maximal contraction). Rings that did not elicit adequate and stable contraction to high K^+ were considered as damaged and discarded. After washout, tissues were precontracted with the thromboxane mimetic 9,11-dideoxy-11α,9α-epoxymethanoprostaglandin $F2_\alpha$ (U-46619). Where indicated DPI was added simultaneously with U-46619 to the

Molecular Pharmacology Fast Forward. Published on June 21, 2013 as DOI: 10.1124/mol.113.086835
This article has not been copyedited and formatted. The final version may differ from this version.

preparation. Addition of 0.3 µM DPI slightly increased the vasoconstrictor response to 50 nM U-46619 (102±4% *vs.* 89±2 % (vehicle) of maximal contraction obtained with 100 mM K^+ ($p<0.05$). After a stable tone had been reached (~20 min), cumulative concentration-response curves were established in separate rings with GTN (0.1 nM - 300 µM) or DEA/NO (1 nM - 10 µM). The contractile force corresponding to each agonist concentration was recorded and is expressed as percent of precontraction.

Determination of NADPH oxidase activity in cultured endothelial cells

Porcine aortic endothelial cells were isolated as described previously (Schmidt et al., 1989) and cultured in 10-cm petri dishes at 37 °C and 5 % CO_2 in Dulbecco's modified Eagle's medium, containing 10 % heat-inactivated fetal calf serum, 100 U/ml penicillin, 0.1 mg/ml streptomycin, and 1.25 µg/ml amphotericin B. Confluent cells were harvested, washed twice with cold phosphate-buffered saline (PBS), resuspended in PBS containing Complete® Protease Inhibitor Cocktail (500 µl per dish) and homogenized by repeated sonication on ice. Protein concentration was measured with the Thermo Scientific Pierce BCA Protein Assay Kit (Fisher Scientific Austria GmbH, Vienna, Austria). Endothelial cell homogenates (0.2 - 0.3 mg of protein) were incubated for 20 min in PBS containing dieethylenetriamine pentaacetic acid (DTPA; 0.1 mM) at 37 °C in the absence or presence of DPI (0.1 - 100 µM) or DIP (1 µM - 1 mM). Subsequently, NADPH (0.3 mM) was added, followed by addition of lucigenin at a non-redox cycling concentration of 5 µM (Li et al., 1998). Lucigenin-derived chemiluminescence was measured every 30 s for 5 min using a TriCarb® 2100TR Liquid Scintillation Counter (Perkin Elmer, Vienna, Austria). Results were corrected for homogenate-deficient blanks and are expressed as percent of controls measured in the absence of DPI or DIP. Lucigenin (N,N'-Dimethyl-9,9'-biacridinium dinitrate) was dissolved in DMSO and diluted in PBS; DPI and DIP were dissolved and diluted in DMSO. The final DMSO concentration in the assays was 1.1 %.

Molecular Pharmacology Fast Forward. Published on June 21, 2013 as DOI: 10.1124/mol.113.086835
This article has not been copyedited and formatted. The final version may differ from this version.

Determination of GTN denitration by purified ALDH2 and ALDH1

The rates of GTN denitration yielding 1,2- and 1,3-GDN were determined as described previously (Kollau et al., 2005). Purified enzymes (ALDH2 or ALDH1, 4 µg each) were incubated with the indicated concentrations of ^{14}C-labeled GTN at 37 °C for 10 min in a final volume of 0.2 ml of 50 mM potassium phoshate buffer, pH 7.4, containing 3 mM $MgCl_2$, 2 mM EDTA, 1 mM NAD^+, 0.1 mM DTPA, 2 mM dithiothreitol (DTT) and 1 % DMSO, latter as vehicle control for DPI. For GTN concentrations ≥ 10 µM, unlabelled GTN was added as required to [^{14}C]GTN. The amount of ^{14}C-labeled GTN was increased to 4 µM for ≥ 30 µM and to 6 µM for 0.2 mM total GTN to increase sensitivity of the assay. Reaction products were extracted twice with 1 ml of diethyl ether, separated by thin layer chromatography, and quantified by liquid scintillation counting. Blank values were determined in the absence of protein under identical conditions and subtracted.

Determination of dehydrogenase activities of ALDH2, ALDH1, and ADH

The dehydrogenase activities of ALDH2 (33 µg/ml), ALDH1 (50 µg/ml) and ADH (0.5 µg/ml) were measured spectrophotometrically as conversion of NAD^+ (0.4 mM) to NADH in the presence of 0.4 mM acetaldehyde (for ALDH1 and ALDH2) or 2 mM ethanol (for ADH) by monitoring the increase in absorbance at 340 nm (ε_{340} = 6.22 mM^{-1} cm^{-1}) at 25 °C (Klyosov et al., 1996) in 50 mM potassium phosphate buffer (pH 7.5), containing 10 mM $MgCl_2$ (only with ALDH isoforms) and 1 % DMSO in the absence or presence of DPI or DIP as indicated.

Determination of the esterase activity of ALDH2

Esterase activity of ALDH2 (6.6 µg/ml) was measured by monitoring the formation of p-nitrophenolate from p-nitrophenyl acetate (pNPA, 0.1 or 0.4 mM) at 400 nm (ε_{400} = 16 mM^{-1} cm^{-1}) at 37 °C in 50 mM potassium phosphate buffer (pH 7.5), containing 10 mM $MgCl_2$ and 1 mM NAD^+. Enzyme concentration was varied to obtain linear increase in absorbance over time as well as appropriate extinction values.

Molecular Pharmacology Fast Forward. Published on June 21, 2013 as DOI: 10.1124/mol.113.086835
This article has not been copyedited and formatted. The final version may differ from this version.

ALDH2-catalyzed bioactivation of GTN measured as activation of purified sGC

Activation of purified sGC (50 ng) by increasing concentrations of GTN (1 nM - 440 µM) was determined by incubation of 4 µg of purified ALDH2 at 37 °C for 10 min in the presence of 0.5 mM [α-^{32}P]GTP (~250,000 cpm), 1 mM NAD^+ and 1,000 U/ml superoxide dismutase as described previously (Beretta et al., 2010; Wenzl et al., 2009a; Wenzl et al., 2011). DPI was present at the indicated concentrations (0.01-100 µM), and DEA/NO (1 µM) served as control for maximal sGC activity. Results were corrected for enzyme-deficient blanks and are expressed as µmol cGMP x min^{-1} x mg^{-1}.

Molecular modeling of DPI and DIP binding

Molecular models of DPI and DIP were docked into the structure of ALDH2 using the Schrodinger software package. Coordinates of ALDH2 were taken from the PDB (pdb-code: 1O02, chain A). The protein was prepared for docking using the protein preparation wizard, followed by deletion of all waters, ions, and ligands. Substrate models were built with the 2D Sketcher of Maestro and optimized with Jaguar. The receptor grid was generated with the ligand diameter midpoint (or “inner”) box centered on Cys-302 (with dimensions of 14 Å in all three directions) and all rotatable groups were treated flexible. Default values were used for all other parameters. Docking was performed in the XP precision mode and using the option for enhancing planarity of conjugated π-systems.

Poses of the ligand were clustered with an r.m.s. tolerance of 0.25 Å. To test whether a binding mode would be observed if the inner box were restricted to the cofactor binding pocket, calculations were repeated with the box centered on the midpoint of residues Thr-244, Gly-245, and Phe-401.

Molecular Pharmacology Fast Forward. Published on June 21, 2013 as DOI: 10.1124/mol.113.086835
This article has not been copyedited and formatted. The final version may differ from this version.

Analysis of enzyme kinetic data

Enzyme kinetic parameters (V_{max} and K_m) were determined in two ways. Plots of enzyme activity against the substrate concentration (v *vs.* [S]) were fitted to the Michaelis-Menten equation $v = V_{max} \bullet [S]/(K_m+[S])$. Alternatively, Lineweaver-Burk plots (1/v vs. 1/[S]) were drawn and the parameters were obtained by weighting the data as described (de Levie, 1986). In both cases each set of experiments (one series of substrate concentrations) was fitted separately; parameters from all sets were averaged and are presented with standard error.

Statistical analysis

Data are presented as mean values ± SEM of n experiments. Concentration-response curves established with different ring segments from a single animal were averaged and counted as individual experiment (n=1). Individual concentration-response curves were fitted to a Hill-type model giving estimates of agonist potency (EC_{50}) and efficacy (E_{max}). Analysis of variance (ANOVA) with post hoc Bonferroni-Dunn test was used for comparison between groups using StatView® (Version 5.0). Significance was assumed at $P<0.05$.

Molecular Pharmacology Fast Forward. Published on June 21, 2013 as DOI: 10.1124/mol.113.086835
This article has not been copyedited and formatted. The final version may differ from this version.

Results

The potency of DPI and DIP to inhibit NADPH oxidase was confirmed by measuring NADPH-induced superoxide generation by endothelial cells as lucigenin fluorescence. As shown in **Fig. 1**, apparent superoxide formation was inhibited by DPI and DIP with IC_{50} values of 0.64±0.20 and 24±9 µM, respectively, a finding that agrees well with previous reports on inhibition of NADPH oxidase in neutrophils and macrophages by these compounds (Hancock and Jones, 1987).

Figure 2A shows that GTN caused biphasic relaxation of rat aortic rings. The high affinity pathway (0.1 nM - 3 µM) exhibited an EC_{50} of 67.5±9.6 nM GTN. In the presence of 0.3 µM DPI, the concentration-response became monophasic with an EC_{50} of 7.1±3.2 µM. Treatment of rats with GTN resulted in nitrate tolerance apparent as impaired relaxation of aortic rings to GTN **(Fig. 2B**). Relaxation of tolerant rings was not further impaired but rather improved by 0.3 µM DPI (EC_{50} = 21.0±8.6 and 5.9±2.0 µM GTN in the absence and presence of DPI, respectively; P=0.16). Relaxation to DEA/NO was not affected by DPI neither in controls nor in nitrate-tolerant vessels **(Fig. 2C, 2D)**. As observed with GTN, DPI showed a tendency to potentiate relaxation of tolerant rings to DEA/NO (Fig. 2D), but the difference in potency of the NO donor was not significant (EC_{50} = 0.16±0.05 and 0.10±0.03 µM in the absence and presence of DPI, respectively; P=0.33). These slight but consistent positive effects of DPI may reflect inhibition of NO scavenging or NADPH oxidase-catalyzed superoxide production. Taken together, the aortic ring experiments suggest that DPI interferes selectively with GTN bioactivation and exhibits an action profile similar to that of established ALDH2 inhibitors.

Assays with purified enzyme confirmed that DPI is a potent inhibitor of ALDH2. **Figure 3A** shows that DPI inhibited ALDH2-catalyzed denitration of GTN to yield 1,2-GDN with an IC_{50} of 0.21±0.04 µM. As we have shown previously, ALDH1 does also

Molecular Pharmacology Fast Forward. Published on June 21, 2013 as DOI: 10.1124/mol.113.086835
This article has not been copyedited and formatted. The final version may differ from this version.

catalyze GTN denitration, albeit with significantly lower affinity (Beretta et al., 2008). Therefore, the effect of DPI on 1,2-GDN formation by ALDH1 was measured in the presence of a 5-fold higher GTN concentration (10 µM). As shown in Fig. 3A, DPI had no effect on the ALDH1-catalyzed reaction at up to 1 µM and caused only about 50 % inhibition at 1 mM, demonstrating that the aryliodonium compound exhibits pronounced ALDH2 selectivity.

The effect of DPI decreased with increasing concentrations of GTN, pointing to a substrate-competitive type of inhibition. Analysis of the data according to Lineweaver-Burk (a representative plot is shown in **Fig. 3B**) revealed K_m values of 16.8±2.1 and 172.4±40.7 µM GTN in the absence and presence of 10 µM DPI, respectively. For comparison the data were also fitted to the Michaelis-Menten equation (not shown), resulting in K_m values of 22.3±2.2 and 163.9±41.8 µM GTN with and without DPI, respectively. Interestingly, both fits indicated a slight increase in V_{max} from 37.2±0.4 to 57.4±6.9 nmol and from 37.8±0.1 to 56.2±7.1 nmol 1,2-GDN x min^{-1} x mg^{-1} according to the Lineweaver-Burk and Michaelis-Menten equations, respectively. GTN denitration was not inhibited by up to 0.1 mM of the related compound DIP (data not shown).

Inhibition by DPI was also observed when GTN bioactivation was assayed as activation of sGC in the presence of purified ALDH2 (**Fig. 4A**). DPI had no effect on cGMP formation triggered by 1 µM DEA/NO but inhibited sGC activation by 1 µM GTN with an IC_{50} of 0.20±0.03 µM. **Figure 4B** shows the effect of DPI on cGMP formation in response to increasing concentrations of GTN. Under control conditions, the EC_{50} of GTN was 0.21±0.30 µM. DPI caused an about 100-fold rightward shift of the GTN concentration-response curve, confirming the GTN-competitive effect observed in the denitration assay. Up to 0.1 mM DIP had no effect (data not shown).

Molecular Pharmacology Fast Forward. Published on June 21, 2013 as DOI: 10.1124/mol.113.086835
This article has not been copyedited and formatted. The final version may differ from this version.

The effects of DPI and DIP on the oxidation of acetaldehyde and ethanol were studied with purified ALDH isoenzymes and ADH, respectively. As shown in **Fig. 5A**, DPI inhibited acetaldehyde oxidation by ALDH2 with an IC_{50} of 0.33±0.03 µM, a value that is virtually identical to the potency of the drug in the denitration and sGC assays. In contrast, the ALDH1-catalyzed reaction was only inhibited by ~35 % with an apparent IC_{50} of 6.1±2.2 µM, and ADH activity was not affected at all by up to 0.1 mM DPI. Similarly to GTN denitration and bioactivation, the dehydrogenase activity of ALDH2 was less sensitive to DIP than to DPI. **Figure 5B** shows the effects of DPI (10 µM) and DIP (10 and 100 µM) on the oxidation of 0.1 and 0.4 mM acetaldehyde. Besides demonstrating the higher potency of DPI, the data also point to substrate-competitive inhibition by both aryliodonium compounds.

GTN denitration is thought to correlate with the esterase activity of ALDH2. To test for inhibition by DPI we measured hydrolysis of pNPA by purified ALDH2. As shown in **Fig. 5C**, DPI inhibited the esterase activity of the enzyme measured in the presence of 0.1 and 0.4 mM pNPA with IC_{50} values of 0.10±0.02 and 0.39±0.09 µM, respectively. Again, activity was only marginally inhibited by up to 0.1 mM DIP (**Fig. 5D**).

High-affinity binding of DPI to ALDH2 was confirmed by molecular modeling. Docking of DPI to ALDH2 with the inner box centered on Cys-302 revealed one binding mode for DPI (**Fig. 6A**) with a docking score of -9.1 kcal/mol. The inhibitor was bound to the active site through van der Waals interactions with Val-120, Met-124, Leu-173, Trp-177, and Phe-296 and polar interactions with Cys-301, Cys-303, and Asp-457. Notably, the ring system was sandwiched between Phe-459 and Phe-170, favouring π-stacking interactions. Superposition with the crystal structure of ALDH2 in complex with GTN (pdb-code: 4fr8) clearly showed overlapping binding sites for the organic nitrate and DPI (**Fig. 6B**). Docking of DIP revealed two solutions with a similar binding mode as observed for DPI but with lower docking scores (-7.2 and -5.8 kcal/mol; data not shown), a finding that agrees well with the significantly lower potency of DIP observed in enzyme assays.

Molecular Pharmacology Fast Forward. Published on June 21, 2013 as DOI: 10.1124/mol.113.086835
This article has not been copyedited and formatted. The final version may differ from this version.

Discussion

The effects of the aryliodonium compounds DPI and DIP have almost exclusively been attributed to interference with flavin-mediated catalysis, in particular the NADPH oxidase reaction. According to a detailed study of the underlying mechanism, inhibition of NADPH oxidases by DPI is mechanism-based, involving electron abstraction from the redox center of the enzyme yielding a reactive phenyl radical that forms a covalent adduct with the flavin cofactor (O'Donnell et al., 1993). In addition to flavin prosthetic groups, metal-bound porphyrins were identified as targets of aryliodonium compounds, suggesting that modification of flavocytochrome *b* may contribute to NADPH oxidase inhibition (Doussiere et al., 1999). Mechanism-based modification of flavin or heme prosthetic groups explains inhibition by DPI of a wide variety of flavoproteins, including NADH:ubiquinone oxidoreductase, NO synthases, xanthine oxidase, cytochrome P450 reductase [see (Aldieri et al., 2008) for review], and aldehyde oxidase (Kundu et al., 2012).

There are several reports on non-flavoproteins that are inhibited by 10 - 100 µM DPI, including metabolic enzymes and ion channels (Aldieri et al., 2008). However, the present study appears to be unique in the identification of a non-flavoprotein with high DPI affinity. In fact, the average IC_{50} values of 0.2 - 0.5 µM that we determined in the various enzyme assays are in the same range or even lower than the inhibitory constants that were reported for inhibition of NADPH and xanthine oxidases [0.3 - 5.6 µM; (Aldieri et al., 2008)]. Inducible NO synthase is the sole target described so far that is even more sensitive to DPI (IC_{50} ~50 nM) (Stuehr et al., 1991). The effects of DPI on denitration and bioactivation of GTN as well as inhibition of ester hydrolysis were clearly substrate-competitive, and the experimental data agree well with molecular modeling, indicating overlapping binding sites for DPI and GTN in the catalytic center of the enzyme (cf. Fig. 6).

Molecular Pharmacology Fast Forward. Published on June 21, 2013 as DOI: 10.1124/mol.113.086835
This article has not been copyedited and formatted. The final version may differ from this version.

Our aortic ring experiments confirm earlier studies from the Bennett laboratory showing that DPI inhibits GTN-induced vasodilation without affecting relaxation to NO (McGuire et al., 1994; McGuire et al., 1998). The effect of DPI has been taken as evidence for the essential involvement of a flavoprotein, in particular cytochrome P450 reductase, in the vascular bioactivation of GTN. So far these data have not been reconciled with the widely accepted role of ALDH2 as the key enzyme catalyzing the high-affinity pathway of GTN-induced relaxation (Chen and Stamler, 2006; Mayer and Beretta, 2008; Münzel et al., 2011). The identification of DPI as potent ALDH2 inhibitor explains the previous observations and provides another piece of evidence for the essential involvement of ALDH2 in GTN vasoactivity. Similar to established ALDH2 inhibitors (Sydow et al., 2004; Wenzl et al., 2009b; Wölkart et al., 2008), DPI had no effect on GTN-induced relaxation of aortic rings from nitrate-tolerant rats (cf. Fig. 2B), further supporting ALDH2 inactivation as key mechanism of GTN tolerance. However, Bennett and coworkers reported that DPI markedly inhibited the GTN response of nitrate-tolerant rat aorta (Ratz et al., 2000). Since the Bennett laboratory has later published similarly conflicting data on the effects of established ALDH2 inhibitors (DiFabio et al., 2003), the controversy could be related to different *in vivo* models of nitrate tolerance.

According to a report from Horowitz and coworkers (De La Lande et al., 1996), DPI has no effect on GTN-induced relaxation of bovine coronary arteries. We re-investigated this issue with porcine coronary arteries and found that these vessels, in contrast to human coronary arteries (Beretta et al., 2012), express only minor amounts of ALDH2 and dilate to GTN in a monophasic, chloral hydrate-insensitive manner, suggesting an ALDH2-unrelated mechanism of GTN bioactivation in certain blood vessels (unpublished observations). Although we have not studied bovine coronary arteries, our observations with the porcine vessels suggest that low ALDH2 expression levels explain the observations published by De La Lande et al. (1996). However, in that paper is has also been shown that DPI even slightly increased the

Molecular Pharmacology Fast Forward. Published on June 21, 2013 as DOI: 10.1124/mol.113.086835
This article has not been copyedited and formatted. The final version may differ from this version.

potency of GTN in bovine vessels with endothelium. This could reflect increased bioavailability of NO due to inhibiton of NO scavenging, an additional effect of DPI (unpublished observation) that is masked in rodent blood vessels by the pronounced inhibition of ALDH2. In any case, DPI appears to be a reliable tool to probe blood vessels for the involvement of ALDH2 in the bioactivation of organic nitrates. Since the drug exhibits pronounced ALDH2 isoform selectivity it may be more useful than established non-selective inhibitors such as chloral hydrate. Higher potency and better solubility may render DPI even more useful than the ALDH2-selective inhibitor daidzin. However, considering the large number of other sensitive targets of DPI, use of this drug should be limited to well-defined *in vitro* set-ups, such as organ bath or cell culture studies testing for the involvement of ALDH2 in the bioactivity of organic nitrates.

Our results may have implications beyond the cardiovascular pharmacology of organic nitrates. A well established function of ALDH2 is oxidation of ethanol-derived acetaldehyde in liver (Svanas and Weiner, 1985). More recently detoxification of reactive aldehydes by ALDH2 has been recognized as important endogenous mechanism that protects the heart from ischemia/reperfusion injury (Chen et al., 2008). In view of the present results it may be necessary to revise some of the earlier conclusions on the involvement of NADPH oxidase activation in cardiovascular disease (Maejima et al., 2011).

Molecular Pharmacology Fast Forward. Published on June 21, 2013 as DOI: 10.1124/mol.113.086835
This article has not been copyedited and formatted. The final version may differ from this version.

Authorship Contributions

Participated in Research Design: Schmidt, Wölkart, Gorren, Schrammel, Mayer

Conducted experiments: R. Neubauer, A. Neubauer, Schwarzenegger, Wölkart

Contributed new reagents or analytic tools: Russwurm, Koesling

Performed data analysis: R. Neubauer, A. Neubauer, Wölkart, Schwarzenegger, Lang, Gorren

Wrote or contributed to the writing of the manuscript: R. Neubauer, A. Neubauer, Wölkart, Schwarzenegger, Lang, Schmidt, Gorren, Schrammel, Mayer

Molecular Pharmacology Fast Forward. Published on June 21, 2013 as DOI: 10.1124/mol.113.086835
This article has not been copyedited and formatted. The final version may differ from this version.

References

Aldieri E, Riganti C, Polimeni M, Gazzano E, Lussiana C, Campia I and Ghigo D (2008) Classical inhibitors of NOX NAD(P)H oxidases are not specific. *Current Drug Metabolism* **9**:686-696.

Beretta M, Gorren ACF, Wenzl MV, Weis R, Russwurm M, Koesling D, Schmidt K and Mayer B (2010) Characterization of the East Asian variant of aldehyde dehydrogenase-2: Bioactivation of nitroglycerin and effects of Alda-1. *J Biol Chem* **285**:943-952.

Beretta M, Gruber K, Kollau A, Russwurm M, Koesling D, Goessler W, Keung WM, Schmidt K and Mayer B (2008) Bioactivation of nitroglycerin by purified mitochondrial and cytosolic aldehyde dehydrogenases. *J Biol Chem* **283**: 17873-17880.

Beretta M, Wölkart G, Schernthaner M, Griesberger M, Neubauer R, Schmidt K, Sacherer M, Heinzel FR, Kohlwein SD and Mayer B (2012) Vascular bioactivation of nitroglycerin is catalyzed by cytosolic aldehyde dehydrogenase-2. *Circ Res* **110**:385-393.

Chen CH, Budas GR, Churchill EN, Disatnik MH, Hurley TD and Mochly-Rosen D (2008) Activation of aldehyde dehydrogenase-2 reduces ischemic damage to the heart. *Science* **321**:1493-1495.

Chen Z, Foster MW, Zhang J, Mao L, Rockman HA, Kawamoto T, Kitagawa K, Nakayama KI, Hess DT and Stamler JS (2005) An essential role for mitochondrial aldehyde dehydrogenase in nitroglycerin bioactivation. *Proc Natl Acad Sci USA* **102**:12159-12164.

Chen Z and Stamler JS (2006) Bioactivation of nitroglycerin by the mitochondrial aldehyde dehydrogenase. *Trends Cardiovasc Med* **16**:259-265.

Chen Z, Zhang J and Stamler JS (2002) Identification of the enzymatic mechanism of nitroglycerin bioactivation. *Proc Natl Acad Sci USA* **99**:8306-8311.

D'Souza Y, Dowlatshahi S and Bennett BM (2011) Changes in aldehyde dehydrogenase 2 expression in rat blood vessels during glyceryl trinitrate tolerance development and reversal. *Br J Pharmacol* **164**:632-643.

De La Lande IS, Philp T, Stafford I and Horowitz JD (1996) Lack of inhibition of glyceryl trinitrate by diphenyleneiodonium in bovine coronary artery. *Eur J Pharmacol* **314**:347-350.

de Levie R (1986) When, why, and how to use weighted least squares. *J Chem Educ* **63**:10-15.

DiFabio J, Yanbin J, Vasiliou V, Thatcher RJ and Bennett BM (2003) Role of mitochondrial aldehyde dehydrogenase in nitrate tolerance. *Mol Pharmacol* **64**:1109-1116.

Doussiere J, Gaillard J and Vignais PV (1999) The heme component of the neutrophil NADPH oxidase complex is a target for aryliodonium compounds. *Biochemistry* **38**:3694-3703.

Fung HL (2004) Biochemical mechanism of nitroglycerin action and tolerance: is this old mystery solved? *Annu Rev Pharmacol Toxicol* **44**:67-85.

Hancock JT and Jones OTG (1987) The inhibition of diphenyleneiodonium and its analogues of superoxide generation by macrophages. *Biochem J* **242**:103-107.

Klyosov AA, Rashkovetsky LG, Tahir MK and Keung WM (1996) Possible role of liver cytosolic and mitochondrial aldehyde dehydrogenases in acetaldehyde metabolism. *Biochemistry* **35**:4445-4456.

Kollau A, Hofer A, Russwurm M, Koesling D, Keung WM, Schmidt K, Brunner F and Mayer B (2005) Contribution of aldehyde dehydrogenase to mitochondrial bioactivation of nitroglycerin: evidence for the activation of purified soluble guanylate cyclase through direct formation of nitric oxide. *Biochem J* **385**:769-777.

Kundu TK, Velayutham M and Zweier JL (2012) Aldehyde oxidase functions as a superoxide generating NADH oxidase: An important redox regulated pathway of cellular oxygen radical formation. *Biochemistry* **51**:2930-2939.

Li Y, Zhu H, Kuppusamy P, Roubaud V, Zweier JL and Trush MA (1998) Validation of lucigenin (bis-N-methylacridinium) as a chemilumigenic probe for detecting superoxide anion radical production by enzymatic and cellular systems. *J Biol Chem* **273**:2015-2023.

Maejima Y, Kuroda J, Matsushima S, Ago T and Sadoshima J (2011) Regulation of myocardial growth and death by NADPH oxidase. *J Mol Cell Cardiol* **50**:408-416.

Mayer B and Beretta M (2008) The enigma of nitroglycerin bioactivation and nitrate tolerance: News, views, and troubles. *Br J Pharmacol* **155**:170-184.

McGuire JJ, Anderson DJ and Bennett BM (1994) Inhibition of the biotransformation and pharmacological actions of glyceryl trinitrate by the flavoprotein inhibitor, diphenyleneiodonium sulfate. *J Pharmacol Exp Ther* **271**:708-714.

McGuire JJ, Anderson DJ, McDonald BJ, Narayanasami R and Bennett BM (1998) Inhibition of NADPH-cytochrome P450 reductase and glyceryl trinitrate biotransformation by diphenyleneiodonium sulfate. *Biochem Pharmacol* **56**:881-893.

Münzel T, Daiber A and Gori T (2011) Nitrate therapy: New aspects concerning molecular action and tolerance. *Circulation* **123**:2132-2144.

O'Donnell VB, Tew DG, Jones OTG and England PJ (1993) Studies on the inhibitory mechanism of iodonium compounds with special reference to neutrophil NADPH oxidase. *Biochem J* **290**:41-49.

Ratz JD, McGuire JJ, Anderson DJ and Bennett BM (2000) Effects of the flavoprotein inhibitor, diphenyleneiodonium sulfate, on ex vivo organic nitrate tolerance in the rat. *J Pharmacol Exp Ther* **293**:569-577.

Russwurm M and Koesling D (2005) Purification and characterization of NO-sensitive guanylyl cyclase. *Methods Enzymol* **396**:492-501.

Schmidt K, Mayer B and Kukovetz WR (1989) Effect of calcium on endothelium-derived relaxing factor formation and cGMP levels in endothelial cells. *Eur J Pharmacol* **170**:157-166.

Stuehr DJ, Fasehun OA, Kwon NS, Gross SS, Gonzalez JA, Levi R and Nathan CF (1991) Inhibition of macrophage and endothelial cell nitric oxide synthase by diphenyleneiodonium and its analogs. *FASEB J* **5**:98-103.

Svanas GW and Weiner H (1985) Aldehyde dehydrogenase activity as the rate-limiting factor for acetaldehyde metabolism in rat liver. *Arch Biochem Biophys* **236**:36-46.

Sydow K, Daiber A, Oelze M, Chen ZP, August M, Wendt M, Ullrich V, Mülsch A, Schulz E, Keaney JF, Stamler JS and Münzel T (2004) Central role of mitochondrial aldehyde dehydrogenase and reactive oxygen species in nitroglycerin tolerance. *J Clin Invest* **113**:482-489.

Tew DG (1993) Inhibition of cytochrome P450 reductase by the diphenyliodonium cation. Kinetic analysis and covalent modifications. *Biochemistry* **32**:10209-10215.

Wenzel P, Müller J, Zurmeyer S, Schuhmacher S, Schulz E, Oelze M, Pautz A, Kawamoto T, Wojnowski L, Kleinert H, Münzel T and Daiber A (2008) ALDH-2 deficiency increases cardiovascular oxidative stress---Evidence for indirect antioxidative properties. *Biochem Biophys Res Commun* **367**:137-143.

Wenzl MV, Beretta M, Gorren ACF, Zeller A, Baral PK, Gruber K, Russwurm M, Koesling D, Schmidt K and Mayer B (2009a) Role of the general base Glu-268 in nitroglycerin bioactivation and superoxide formation by aldehyde dehydrogenase-2. *J Biol Chem* **284**:19878-19886.

Wenzl MV, Beretta M, Griesberger M, Russwurm M, Koesling D, Schmidt K, Mayer B and Gorren ACF (2011) Site-directed mutagenesis of aldehyde dehydrogenase-2 suggests three distinct pathways of nitroglycerin biotransformation. *Mol Pharmacol* **80**:258-266.

Wenzl MV, Wölkart G, Stessel H, Beretta M, Schmidt K and Mayer B (2009b) Different effects of ascorbate deprivation and classical vascular nitrate tolerance on aldehyde dehydrogenase-catalysed bioactivation of nitroglycerin. *Br J Pharmacol* **156**:1248-1255.

Wölkart G, Wenzl MV, Beretta M, Stessel H, Schmidt K and Mayer B (2008) Vascular tolerance to nitroglycerin in ascorbate deficiency. *Cardiovasc Res* **79**:304-312.

Zheng CF, Wang TT and Weiner H (1993) Cloning and expression of the full-length cDNAS encoding human liver class 1 and class 2 aldehyde dehydrogenase. *Alcohol Clin Exp Res* **17**:828-831.

Molecular Pharmacology Fast Forward. Published on June 21, 2013 as DOI: 10.1124/mol.113.086835
This article has not been copyedited and formatted. The final version may differ from this version.

Footnotes

This work was supported by the Austrian Science Fund [P24946, P23135] and by the Deutsche Forschungsgemeinschaft [KO1157/4-1].

Molecular Pharmacology Fast Forward. Published on June 21, 2013 as DOI: 10.1124/mol.113.086835
This article has not been copyedited and formatted. The final version may differ from this version.

Legends for figures

Fig.1. Effects of DPI and DIP on NADPH-dependent lucigenin fluorescence in cultured porcine aortic endothelial cells. Cell homogenates (0.2 - 0.3 mg of protein) were incubated at 37 °C for 20 min with increasing concentrations DPI or DIP (1 µM - 1 mM). Reactions were started by addition of NADPH and lucigenin (0.3 mM and 5 µM final, respectively). Chemiluminescence was measured every 30 s for 5 min in a Liquid Scintillation Counter. Data (mean values ± SEM of three independent experiments) are expressed as percent of controls measured in the absence of DPI and DIP.

Fig. 2. Effects of DPI on relaxation of aortic rings to GTN and DEA/NO. Rings obtained from control (A, C) or nitrate-tolerant (B, D) rats were precontracted with the thromboxane mimetic U-46619 (50 nM) in the absence (open circles) or presence (filled circles) of 0.3 µM DPI, and cumulative concentration-response curves to GTN (A, B) or DEA/NO (C, D) were established. Data obtained with two different ring segments from the same rat (either untreated or nitrate-tolerant) were averaged and counted as individual experiment (n=1). The results shown are mean values ± S.E.M. of three experiments, i.e. 6 rings from three rats.

Molecular Pharmacology Fast Forward. Published on June 21, 2013 as DOI: 10.1124/mol.113.086835
This article has not been copyedited and formatted. The final version may differ from this version.

Fig. 3. Effects of DPI on GTN denitration catalyzed by purified ALDH isoforms. Purified ALDH proteins (4 µg each) were incubated with [^{14}C]GTN at 37 °C for 10 min in 0.2 ml of 50 mM potassium phosphate buffer, pH 7.4, containing 3 mM $MgCl_2$, 2 mM EDTA, 1 mM NAD^+, 0.1 mM DTPA, and 2 mM DTT. 1,2-GDN was extracted and analyzed by TLC as described under "Materials and Methods". **A:** Reactions were carried out with 2 µM [^{14}C]GTN in the presence of the indicated concentrations of DPI. Data are mean values ± S.E.M. of three independent experiments. B: Lineweaver-Burk plot of the denitration activity of ALDH2 determined with increasing concentrations of [^{14}C]GTN (2 - 200 µM) in the absence or presence of 10 µM DPI. The plot shown is representative for three similar experiments.

Fig. 4. Effects of DPI on GTN-triggered activation of purified sGC in the presence of purified ALDH2. Purified sGC (50 ng) was incubated at 37°C for 10 min with 4 µg of ALDH2 in the presence of 0.5 mM [α-^{32}P]GTP (~250,000 cpm), 1,000 units/ml SOD, and 1 mM NAD^+ with DPI, GTN or DEA/NO as indiacted, followed by isolation of ^{32}P-cGMP and determination of radioactivity by liquid scintillation counting. **A:** Effects of the indicated concentrations of DPI on sGC activity determined in the presence of GTN or DEA/NO (1 µM each). **B:** Activation of sGC by increasing concentrations of GTN in the absnece and presence of 10 µM DPI. The data are mean values ± S.E.M. of 3-4 independent experiments performed in duplicate.

Molecular Pharmacology Fast Forward. Published on June 21, 2013 as DOI: 10.1124/mol.113.086835
This article has not been copyedited and formatted. The final version may differ from this version.

Fig. 5. Effects of DPI and DIP on dehydrogenase and esterase activities. Dehydrogenase activity (A, B) was measured photometrically with 0.1 - 0.4 mM acetaldehyde (AcCOH; ALDH1 and ALDH2) or 2 mM ethanol (ADH), and the esterase activity of ALDH2 (C,D) was determined in the presence of 0.1 - 0.4 mM pNPA. See “Materials and Methods” for description of the assays. **A:** Effects of increasing concentrations of DPI on the oxidation of 0.4 mM acetaldehyde (ALDH2 and ALDH1) or 2 mM ethanol (ADH). **B:** Effect of DIP compared to DPI in the presence of two different concentrations of acetaldehyde. **C:** Effects of increasing concentrations of DPI on the hydrolysis of 0.1 and 0.4 mM pNPA. **D:** Effect of DIP compared to DPI on the hydrolysis of 0.1 mM pNPA. Data are mean values ± S.E.M. of 3-6 independent experiments.

Fig. 6. Model of DPI binding to ALDH2

A: Stereoscopic representation of the active site of ALDH2 (green) in complex with DPI (blue). The enzyme is shown as cartoon and active site residues and DPI are shown as sticks.

B: Superposition of the modelled ALDH2-complex with DPI and the experimentally determined structure of GTN-bound ALDH2 (pdb-code 4fr8). The enzyme is shown as cartoon (green), Cys-302, DPI (blue), and GTN (red) are shown as sticks.

Molecular Pharmacology Fast Forward. Published on June 21, 2013 as DOI: 10.1124/mol.113.086835
This article has not been copyedited and formatted. The final version may differ from this version.

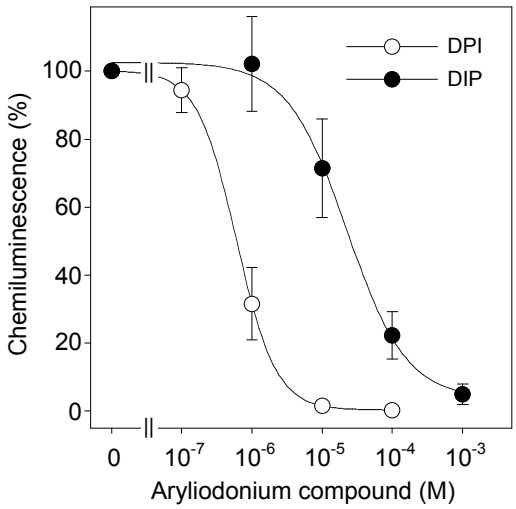

Fig. 1

Molecular Pharmacology Fast Forward. Published on June 21, 2013 as DOI: 10.1124/mol.113.086835
This article has not been copyedited and formatted. The final version may differ from this version.

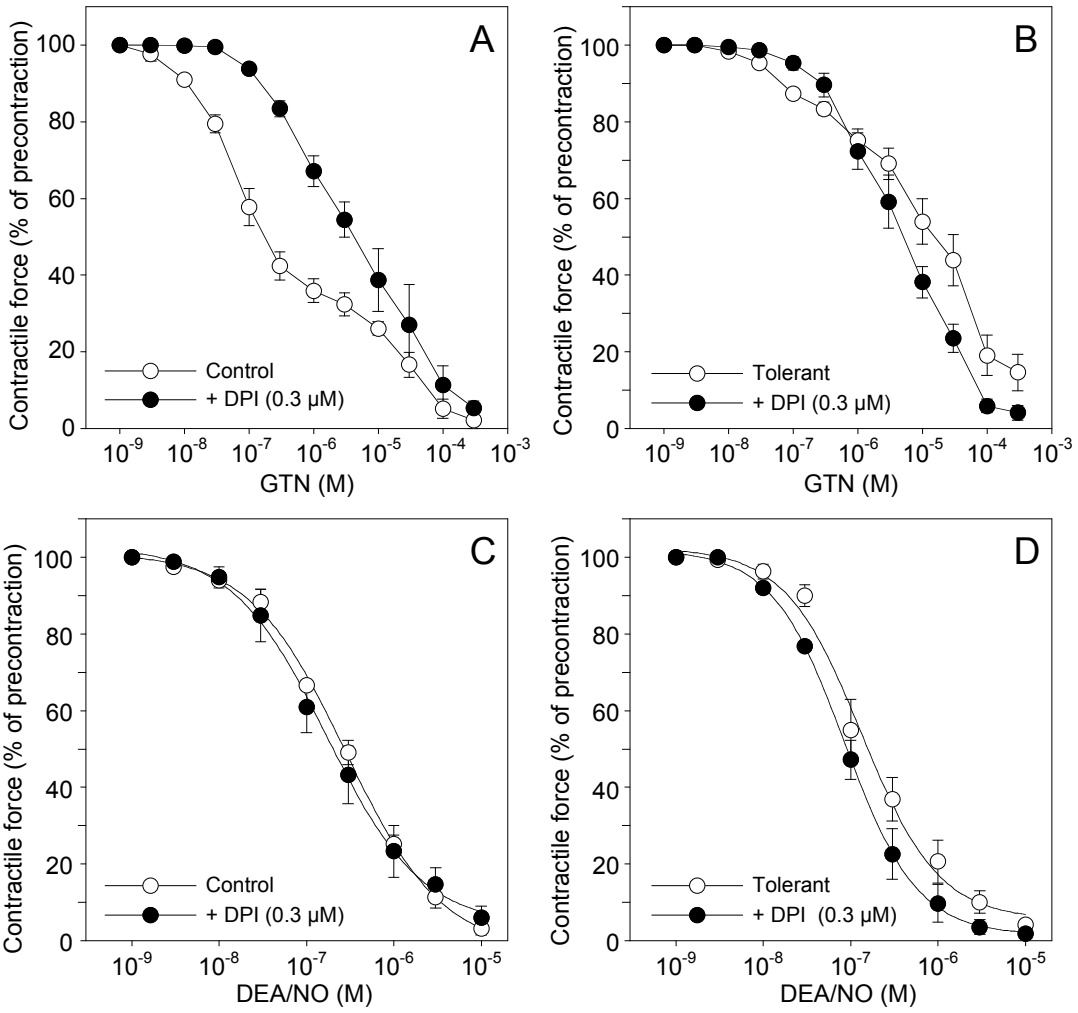

Fig. 2

Molecular Pharmacology Fast Forward. Published on June 21, 2013 as DOI: 10.1124/mol.113.086835
This article has not been copyedited and formatted. The final version may differ from this version.

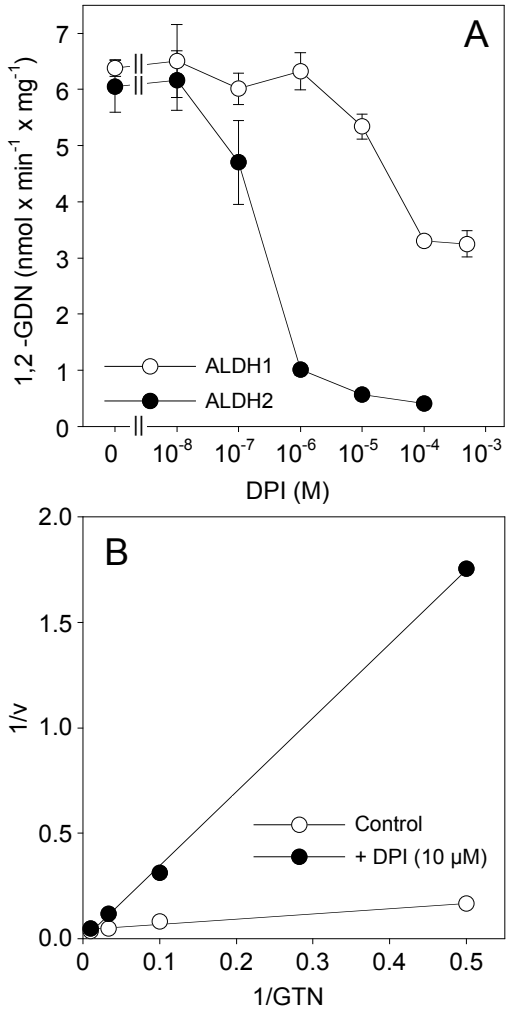

Fig. 3

Molecular Pharmacology Fast Forward. Published on June 21, 2013 as DOI: 10.1124/mol.113.086835
This article has not been copyedited and formatted. The final version may differ from this version.

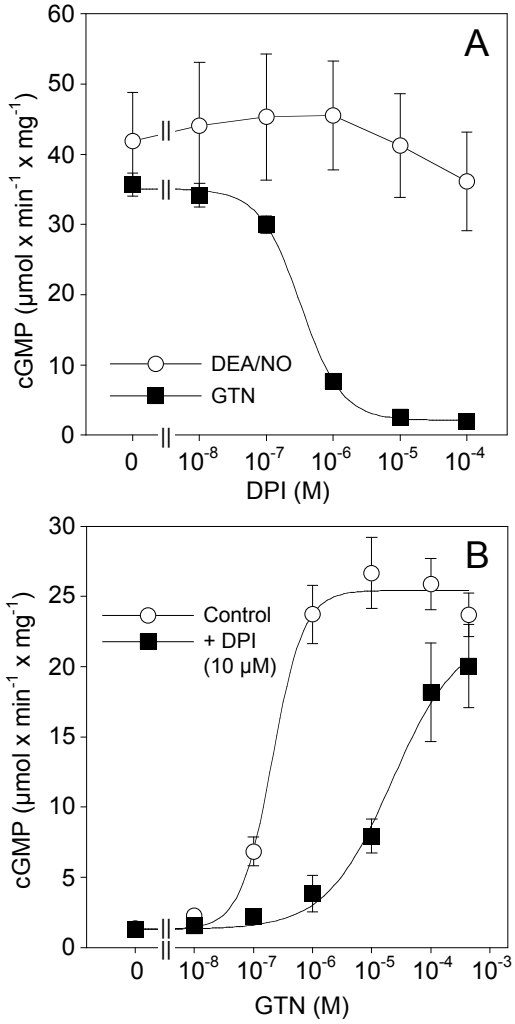

Fig. 4

Molecular Pharmacology Fast Forward. Published on June 21, 2013 as DOI: 10.1124/mol.113.086835
This article has not been copyedited and formatted. The final version may differ from this version.

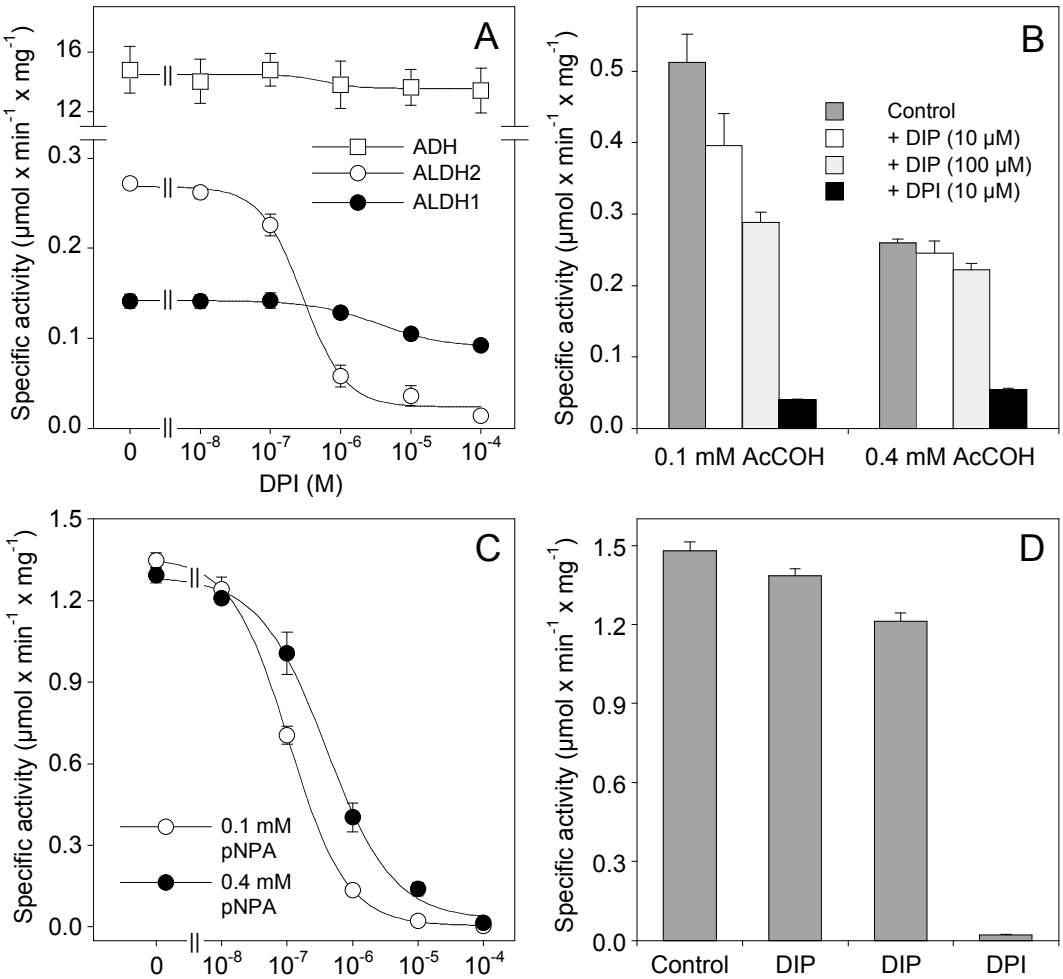

Fig. 5

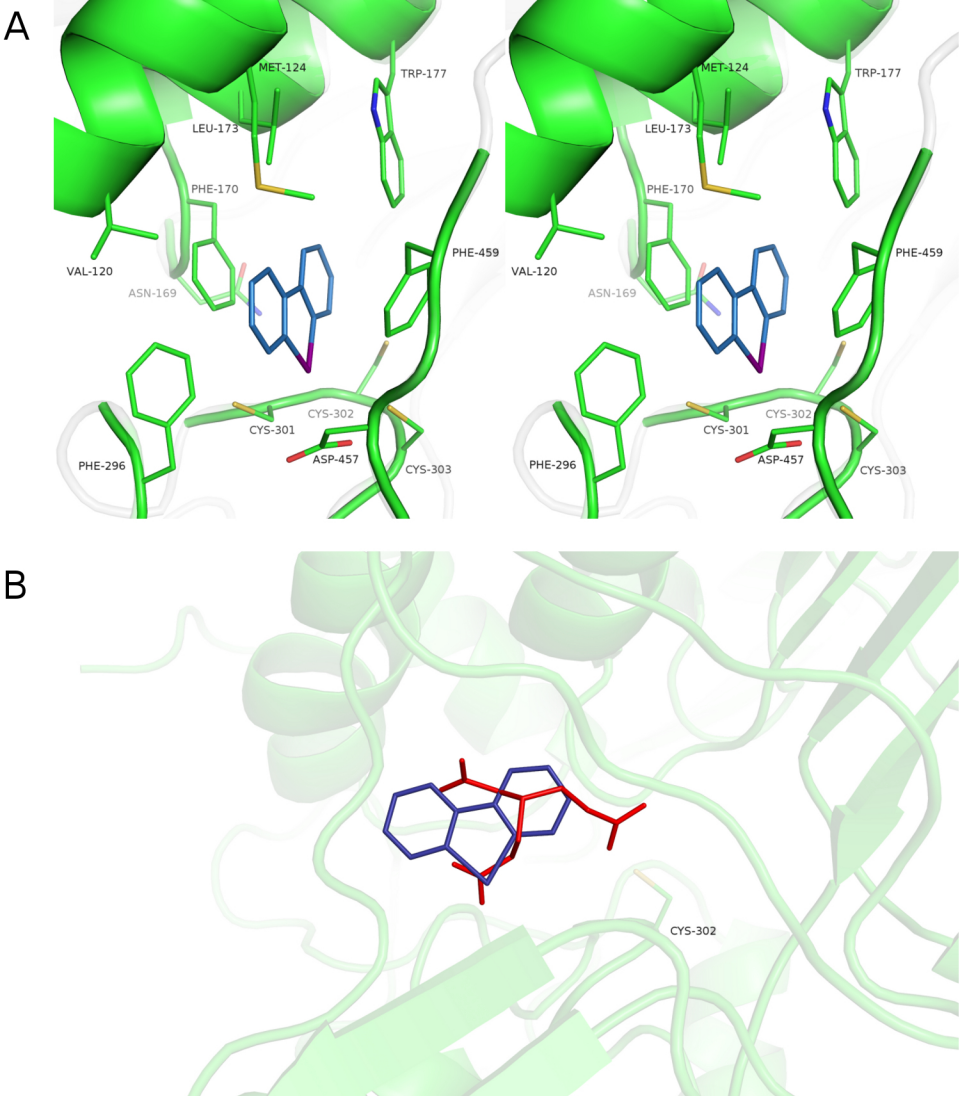
A
MET-124
TRP-177
LEU-173
PHE-170
VAL-120
ASN-169
PHE-459
CYS-302
CYS-301
PHE-296
ASP-457
CYS-303
MET-124
TRP-177
LEU-173
PHE-170
VAL-120
ASN-169
PHE-459
CYS-302
CYS-301
PHE-296
ASP-457
CYS-303
B
CYS-302

Fig. 6